FOREWORD

This report was prepared by the Metals Research Laboratory, Division of Applied Mathematics, Brown University, Providence, Rhode Island under USAF Contract No. AF 33 (616)-6945. This contract was initiated under Project No. 7360 "Research to Investigate the Use of Ultrasonic Methods in the Study of Deformation and Fatigue in Materials," Task No. 736002 "Nondestructive Testing." The work was administered under the direction of the Directorate of Materials and Processes, Deputy for Technology, Aeronautical Systems Division, with Mr. R. R. Rowand acting as the project engineer.

This report covers work conducted from December 1960 to December 1961.

We are indebted to Mr. Richard Rowand for direct assistance and for appreciation of the difficulties associated with this work as well as the results.
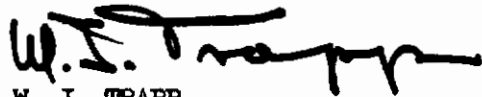
ABSTRACT

The use of ultrasonic methods for studying defect formation and its consequences in connection with stress cycling and deformation in aluminum and sodium chloride single crystals is the subject of this report.

The observed ultrasonic changes appeared closely associated with changes in dislocation behavior. To establish this deformation experiments were used in such a way that results could be related to the behavior of the slip systems and to their orientation. Aluminum single crystals were used for these experiments. Simultaneous measurements of attenuation and velocity changes were made continuously during tensile deformation. In the very early stages of deformation, for all orientations, an increase in attenuation is observed before microscopic yield. Easy glide is observed by the attenuation and velocity changes.

Measurements in tension have been made for the purpose of comparing the dislocation damping and pinning effects in an ionic crystal with those in a metal.

Important equipment improvements have been made for automatic recording of attenuation and velocity measurements.

This report has been reviewed and is approved.

W. J. TRAPP
Chief, Strength & Dynamics Branch
Metals and Ceramics Laboratory
Directorate of Materials and Processes

TABLE OF CONTENTS

LIST OF ILLUSTRATIONS

INTRODUCTION

The purpose of this investigation is that of understanding the physical changes which are detected and continuously measured in aluminum and sodium chloride during deformation and stress cycling. The changes in the material are detected and followed by means of the measurement of ultrasonic attenuation and velocity. These measurements are made by pulse echo methods in the very low megacycle range of frequencies. A discussion of the earlier work of this type is given in several articles (1)(2)(3)(4) particularly in articles (3) and (4) which are concerned with attenuation and velocity effects observed in the very early stages of stress cycling between one and 10^4 cycles. An explanation of the observed effects was also provided in these reports.

The present report is concerned with the following topics:

I. Discussion of Measurements and Results Related to the Ultrasonic Attenuation and Velocity Data on Aluminum Single Crystals as a Function of Deformation and Orientation.

II. Discussion and Results Related to the Ultrasonic Attenuation and Velocity Data on Sodium Chloride Single Crystals as a Function of Deformation and Orientation.

III. Stress Cycling

IV. Description of Automatic Recording Velocity Measurement System.

I.   Discussion of Measurements and Results Related to the Ultrasonic Attenuation and Velocity Data on Aluminum Single Crystals as a Function of Deformation and Orientation.

The following account of ultrasonic attenuation and velocity measurements carried out during tensile deformation of high purity single crystal aluminum samples shows, among other things, the close connection between dislocation damping and the easy glide mechanism. Stress-strain measurements made concurrently with attenuation-strain and velocity-strain measurements show from their orientation dependence how the operation of four, six, and eight glide systems affects the dislocation damping hence the attenuation and velocity.

The work described shows how ultrasonic measurements of this type may be used to study the details of slip mechanisms.

Experimental Procedure

The material used throughout this experiment was aluminum 99.995^{+}% pure. Single crystals of 3/8" square in cross section and about 12" long were grown in this laboratory using a graphite boat and pre-oriented seeds. These were so oriented that the long axis of the crystal coincided with the following crystallographic directions $\langle 100 \rangle$, $\langle 110 \rangle$, $\langle 111 \rangle$ and "$\langle 0.5 \rangle$". Here, "$\langle 0.5 \rangle$" orientation means that one of the twelve possible glide systems of the face centered cubic crystal is inclined 45 degrees to the rod axis, so that when the specimen is stressed along that axis, the maximum resolving shear factor of 0.5 is obtained.

Single crystals thus obtained were cut slightly longer than 5 inches in length and glued into a steel holder 5 inches long and with a groove 3/8 inch square along its axis. Since the end surfaces of the holder are made parallel to each other and perpendicular to its axis, the end surfaces of the single crystal can be finished parallel and perpendicular to this axis when the excess length of the crystal was removed.

After polishing the end surfaces, the specimens were annealed at $550^{o}C$ for three hours. Then the specimen was glued into specially designed grips of the testing machine, using Aralite (trademark of CIBA), without tightening or squeezing so that deformation prior to the test is avoided. The grips and alignment of the specimen are shown Schematically in Figure 1.

The specimens were deformed in tension at room temperature using an Instron table model testing machine. The speed of the crosshead movement was 0.002"/min. throughout the experiments. The load was measured by a load cell and recorded as a function of time. The elongation of the specimen was measured by three dial indicators reading to 0.0001" per division. These indicators were arranged in a way shown schematically in Figure 2. These indicators are this way in order to detect and compensate bending deformation and in order to obtain total length change of the specimen instead of elongation between grips, because the velocity change due to deformation

2

was measured by the change in delay time required for ultrasonic waves to make one round trip of the total specimen length.

Changes of attenuation and velocity were determined by the pulse echo technique. The diameter of the transducers used was 0.35 inches. The transducers were mounted on one end of the specimen using Nonaq (Fisher Scientific Co.) as the bonding agent. Since the change of the attenuation due to deformation was unusually large, the ordinary method of measuring attenuation, i.e. matching an exponential decay curve to the echoes, could not be used. Instead, the change of amplitude of the first echo was traced and recorded automatically throughout the deformation process. The velocity change was determined from the measurements of the delay time change of the first echo, together with the measurement of the elongation mentioned above

Instrumentation for these measurements was set up as shown in block diagram form in Figure 3. Attenuation changes were plotted out over a 40 db range by using the attenuation readout adaptor[4] (AARA-I) in a slightly modified configuration. This unit was initially designed to sense the relative change in amplitude of any two ultrasonic echoes. Since the second and all succeeding echoes disappear with increasing strain in this particular type of experiment, it became necessary to introduce an artificial constant amplitude echo and to measure change in attenuation of the first echo with respect to this. The delay trigger output from the Mk XVIII attenuation measurement unit was used as the artificial echo. The AGC system was disabled in this configuration. To obtain greater than 20 db dynamic range a stepped attenuation was inserted in the receiving system at the input to the I.F. strip. At the beginning of an experiment the attenuation in a typical sample was low enough to allow the insertion of 40 db loss in the receiving system. The AARA-I was used on the 10 db scale. When the attenuation in the sample had increased 10 db in the first round trip, 10 db was removed from the path. This could be done 4 times plus the 10 db range of the recorder therefore a total change of 50 db could be plotted. Changes in round trip time in the sample were obtained from the Velocity Readout Adaptor (VERA-I) as indicated in reference [4]. The first echo was necessarily used for this purpose since all later echoes subsequently disappear during an experiment. The amplitude of this first echo is maintained at a constant amplitude by manually adjusting the continuously variable 60 mc/sec attenuator. It is necessary to do this since the velocity Readout Adaptor is sensitive to input amplitude.

Experimental Results

a) ⟨0.5⟩ orientation

Figure 4 shows the relationship between stress, attenuation change and fractional change of velocity against the strain, for 10 MC shear waves. The polarization of the transducer was so oriented that the particle displacement of the vibration was perpendicular to the projection of the primary glide direction into the end surface, as shown in Figure 4. That is, the particle displacement of the vibration does not have any component in the primary glide direction.

3

After the initial rise (stage A) the stress-strain curve clearly indicates the existence of easy glide for approximately 0.2 % tensile strain stage B, followed by stage C*. The corresponding attenuation change (the difference between the attenuation for any particular strain and the initial attenuation at zero strain) is very similar in shape to the stress-strain curve; that is, after an initial rise, the attenuation stays almost unchanged during the easy glide region and then starts to rise and keeps increasing steadily in stage C.

The corresponding velocity change is defined by

$$\frac{\Delta V}{V} = \frac{V(\varepsilon) - V}{V}$$

where V is the initial velocity before the deformation and $V(\varepsilon)$ is the velocity for a particular strain**. As shown in Figure 4, the velocity increased slightly at the beginning, remained practically unchanged during easy glide and then decreased rapidly in stage C.

The behavior of longitudinal waves is different. As shown in Figure 5, the attenuation increases quite rapidly with increasing strain, from the beginning of the deformation, and does not exhibit any special characteristic associated with easy glide. The corresponding velocity change is also different from the shear wave case; after a slight increase in the beginning, it tends to decrease immediately, again without any observed relation to the easy glide.

b) Symmetrical orientations.

The experimental results obtained with 13 MC longitudinal waves for $\langle 100 \rangle$, $\langle 111 \rangle$, and $\langle 110 \rangle$ orientations are shown in Figure 6, Figure 7, and Figure 8 respectively. The results on 10 Mc shear waves for $\langle 100 \rangle$ and $\langle 110 \rangle$ orientations are shown in Figure 9 and Figure 10 respectively. No measurements could be made with shear waves propagating along the $\langle 111 \rangle$ direction, because of a complicated decay pattern.

---

*C is used to designate the portion of the stress-strain curve that follows easy glide, without reference to a specific strain hardening mechanism.

**This $\frac{\Delta V}{V}$ should be distinguished from the theoretical fractional velocity change derived from the expression (2) given in the discussion section, because the theoretical velocity change is the difference between the purely elastic velocity at infinite frequency and the measured velocity at any given strain or frequency.

4

For all these cases, the attenuation increases rapidly from the start of the deformation, and the velocity change shows a definite maximum at around 0.02 ~ 0.1 % strain. The location and the size of the maximum vary for different orientations.

Discussion of the results

The experimental results reported above definitely suggest that the measured changes of attenuation and velocity are associated with dislocation motion. It is therefore of interest to try to interpret the present results in terms of the dislocation damping treatment given by Granato and Lucke[5]. These authors show that the damping of a specimen containing dislocations is described by the logarithmic decrement Δ, given by

$$\Delta = \Omega \Delta_o \Lambda \eta^2 \frac{\omega d}{\left[(\omega_o^2 - \omega^2)^2 + (\omega d)^2\right]} \qquad (1)$$

Since the motion of the dislocation lines produces a strain in addition to the elastic strain, the apparent modulus C is lower than the true modulus G_o, by an amount ΔG, given by

$$\frac{\Delta G}{G_o} = \frac{\Omega \Delta_o \Lambda \eta^2}{\pi} \frac{(\omega_o^2 - \omega^2)}{\left[(\omega_o^2 - \omega^2)^2 + (\omega d)^2\right]} \qquad (2)$$

In the above expressions, the symbols have the following meanings. Total length of movable dislocation line per unit volume Λ, lattice parameter a, circular frequency ω, Poisson's ratio ν. $\Delta_o = 4(1-\nu)/\pi^2$ $d = B/A$, the dislocation mass per unit length $A = \pi \rho b^2$, damping constant B, density ρ, Burgers vector b, $\eta = \pi \sqrt{\frac{C}{A}}$, $C = 2Gb^2/\pi(1-\nu)$ $\omega_o = \eta/L_e$, effective length of dislocation loop L_e, orientation factor Ω.

Since the attenuation α measured in db/μsec is related to the logarithmic decrement Δ by

$$\alpha = 8.68 \times 10^{-6} \left(\frac{\omega}{2\pi}\right) \Delta$$

equation (1) can be rewritten as follows:

$$\alpha = \frac{\Omega \Delta_o \Lambda \eta^2 d \omega^2}{2\pi} \cdot \frac{1}{\left[(\omega_o^2 - \omega^2)^2 + (\omega d)^2\right]} 8.68 \times 10^{-6} \qquad (3)$$

5

The values of A, B and C will be considered constant for the material, and the frequencies of the experiments are fixed at 10 MC or 13 MC, thus the attenuation increases with increasing Ω, Λ and L_e. For a sufficiently small amount of deformation it can be assumed that Ω and Λ remain unchanged, and most of the changes in attenuation and velocity are due to the increase of loop length L_e. For such a case, the attenuation and velocity change are plotted against (ω_o/ω) in Figure 11. Here, the attenuation and fractional velocity change are normalized to their maximum values, and the value $(\frac{d}{\omega})^2 = 10^6$, is used. Since the resonant frequency ω_o is related to the loop length L_e by

$$\omega_o = ^m\!/\!L_e$$

the increase of L_e corresponds to the decrease of ω_o/ω in Figure 11. From this figure, the experimental results on the increase in attenuation as well as in velocity can be explained if the value of ω_o/ω before the deformation is in the range between one (where the maximum takes place in the $\alpha - (\omega_o/\omega)$ curve) and $\cong$ 30 (where the minimum takes place in the $\Delta V/_V - \omega_o/\omega$ curve). Furthermore, from the previous condition it is possible to estimate the upper and lower limits of the loop length for which an increase in both attenuation and velocity can be observed. Figure 12 shows the limits of loop length against the frequency for two different values of B. For the frequency of 13 MC used in these experiments the limits of the loop length given by this estimation become 3.2×10^{-4} cm $< L_e < 8 \times 10^{-3}$ cm, which is reasonable for the purity of the aluminum single crystals used in this experiment.

Thus the increase of the attenuation as well as the velocity in the early stages of deformation can be explained. Furthermore, this consideration provides the explanation for the previous experiments [6] where no velocity increase was observed. In those experiments, less pure aluminum polycrystals were used as specimens and the ultrasonic frequency was 5 MC. Under these conditions, the loop length would be smaller than the lower limit derived above, and a velocity increase effect could not be observed.

The expansion of loop length is limited, for as soon as sufficient dislocation multiplication takes place, the dislocations in different glide systems intersect each other and cause a shortening of the loop length. Therefore, there is a maximum in the $\Delta V/_V$ deformation curves. As can be seen from the expressions (2) and (3), $\Delta V/_V$ is more sensitive to the change of ω_o or loop length, in the range of $(\omega_o/\omega)^2 < d/\omega$, than the attenuation α is. Therefore, the attenuation continues to increase because of the increase of dislocation density even though the velocity decreases.

The location and the size of the maximum in the $\Delta V/_V$ - deformation curve should depend on how soon in the deformation process, sufficient intersections take place. It is natural to assume that among the three symmetrical orientations, sufficient intersection takes place earliest in the $\langle 100 \rangle$ orientation, next in the $\langle 111 \rangle$ orientation, and then in the $\langle 110 \rangle$ orientation, because the $\langle 100 \rangle$, the $\langle 111 \rangle$ and the $\langle 110 \rangle$ orientation have 8, 6 and 4 equally favored glide systems respectively*.

---

* For these orientations the resolved stress is zero on the remaining of the twelve possible slip systems.

6

As shown in Figure 13 where the fractional velocity changes $\Delta V/V$ are plotted against the resolved shear strain, the location and size of the maxima are exactly in the order predicted from the crystallographic orientation considerations mentioned above.

As the deformation increases, the assumption that Ω and Λ remain constant becomes less and less valid. As soon as the dislocation multiplication becomes appreciable the distribution of dislocations on each glide system changes. Therefore the orientation factor* Ω , which depends on the crystallographic orientation of the specimens and the modes of the ultrasonic waves used, is also a function of deformation. However, the change of Ω as a function of plastic strain cannot be computed without further assumptions about the details of dislocation multiplication.

Figure 14 and Figure 15 show the comparison of the attenuation change for the symmetrical orientations obtained at 13 MC longitudinal waves and 10 MC shear waves respectively. The difference in attenuation change with strain for the three symmetrical orientations can also be explained qualitatively on the basis of differences in the change loop length. As mentioned above, sufficient dislocation multiplication causes a shortening of the loop length, and, for larger deformations, the value $(\frac{\omega_o}{\omega})^2$ approaches the value (c/ω). As can be seen from the expression (3), the attenuation becomes more sensitive to the change of loop length in the range of $(\omega_o/\omega)^2 \cong (c/\omega)$. Moreover, the loop length, at a given stage of deformation, is expected to be largest in the $\langle 110 \rangle$ orientation and smallest in the $\langle 100 \rangle$, with intermediate values in the $\langle 111 \rangle$ orientation, thus the difference in attenuation change is also expected to be in that order. This is indeed found to be the case as shown in Figure 15 and Figure 16.

In the case of $\langle 0.5 \rangle$ orientation, the marked difference in the attenuation change between shear waves polarized perpendicularly to the primary slip direction, and longitudinal waves, can be understood in the following way: the $\langle 0.5 \rangle$ orientation is such that only one of the 12 possible $\{111\} \langle 110 \rangle$ glide systems has the maximum resolved shear factor of 0.5 and the rest of the glide systems have smaller resolved shear factors. For such an orientation the onset of macroscopic flow is usually attributed to rapid dislocation multiplication which is confined essentially to the primary slip system. This corresponds to the easy glide region (stage B) in the stress-strain curve. The termination of easy glide is thought to coincide with the stress values for which substantial dislocation multiplication begins to occur in at least one additional slip system, on which dislocations have to travel through the forest of dislocations already developed in stage B. This corresponds to stage C. Since the shear wave is so polarized that the particle displacement of the vibration has components along all the glide systems except the primary one, the shear wave does not "see" the glide motion of dislocations in the primary glide system. Therefore, in the easy glide region, attenuation of the shear wave does not increase. However, in stage C,

---

* Originally derived on the assumption of an isotropic distribution of dislocations.

7

the shear wave begins to detect the effect of additional dislocation multiplication in secondary slip systems, in all of which there is a component of vibrational displacement. This is reflected in a rapid increase in the observed attenuation. Longitudinal waves, however, have components along all the glide systems including the primary one. This explains the experimental fact that the attenuation increases quite rapidly as a function of strain, from the beginning of the deformation, without any relation to the easy glide.

As far as the authors are aware, this is the first experimental separation of the effects of primary and secondary glide systems during plastic deformation of face centered cubic single crystals.

Conclusions

It is shown that the changes of ultrasonic attenuation and velocity in single crystals of aluminum due to plastic deformation, are very sensitive to the orientation of the crystals. For symmetrical orientations, the change of attenuation decreases with the increasing number of equally favored slip systems; i.e. in the order $\langle 110 \rangle$ $\langle 111 \rangle$, $\langle 100 \rangle$ having 4,6 and 8 equally favored slip systems respectively.

In the case of $\langle 0.5 \rangle$ orientation, the change of shear attenuation clearly shows the easy glide phenomenon when the polarization direction is appropriately oriented, while the longitudinal wave attenuation increases, without showing any characteristic connected with easy glide.

The velocity increases slightly in the beginning of deformation and then tends to decrease, that is the $\Delta V\!/\!v$ — deformation curve has maximum. The location and size of the maximum also depend on the crystallographic orientation, in the same way as in the case of the attenuation change.

The increase in velocity as well as attenuation in the early stages of deformation can be explained on the basis of the dislocation damping treatment given by Granato and Lucke, if the loop lengths of the dislocations, before the deformation, are larger than 3.2×10^{-4} cm, taking the damping constant B equal to 5×10^{-4}.

8

II.   Ultrasonic Attenuation and Velocity Data on Sodium Chloride Single Crystals as a Function of Deformation and Orientation.

In the course of the study of dislocation pinning and unpinning that occurs during deformation and during recovery after deformation, it has become apparent that any property of the solid related to dislocation changes is worth investigating because there are a sufficiently large number of variables so that really definitive experiments require several kinds of measurements. It is for this reason that we have been convinced that it is desirable to compare the deformation of metallic crystals (aluminum) with the deformation of ionic crystals. Ionic crystals exhibit large changes in electrical conductivity during deformation. This increase in conductivity disappears in about twenty minutes at room temperature. The point defects are assumed to be associated with both conductivity changes and dislocation pinning hence damping changes. Since a dislocation acts as a source of point defects during deformation and as a sink for point defects during recovery it is certainly worthwhile to examine the connection between the concentration of point defects, as shown by conductivity measurements, and deformation as compared with attenuation and velocity changes.

In addition to conductivity changes there is a "charge effect" in the deformed sodium chloride in which there appears to be a charge associated with dislocations. When the dislocations move the charge effect can be observed at the surface of the sample.

In the deformation experiments carried out in our laboratory the specimens were in the form of rods 3/4 inch in diameter and 4 1/2 inches long (Harshaw Chemical Co.). The orientation of the samples was such that their axis coincided with a $\langle 100 \rangle$ direction of the crystal. The surfaces of the rod specimen were polished with water for the purpose of inhibiting the formation of cracks during deformation.

The specimens were mounted in grips of the Instron Tensile testing machine, and the measurement of attenuation and velocity was carried out in the same way as with the aluminum samples except that with NaCl the sample was glued into the grips with Stycast 2651 (Emerson and Cummings, Inc.). The reason for the difference in the epoxy resins was simply that NaCl could be taken out of the grips by disolving the sample and this could not be done with aluminum hence with the aluminum samples the glue had to have a solvent and with NaCl it did not. Stycast is stronger than the resin used for aluminum but Stycast has no solvent. With NaCl the transducer used was one half inch in diameter.

The results of the deformation of sodium chloride are shown in what follows. Figure (17) shows the dependence of stress, attenuation change, and fractional velocity change on strain for 10 mc/sec compressional waves.

The attenuation and velocity results are quite similar in form to those obtained with aluminum single crystals. The attenuation increases with strain and the velocity change has a maximum at about 0.1% strain although the actual change in $\Delta V/V$ from zero strain to 0.1% strain is much smaller than it is in aluminum.

9

Recovery experiments have been carried out where the load remains on and where the load has been removed. Attenuation and velocity measured as a function of time with and without load are shown in Figure (17). Recovery with the "load on" was measured with constant strain at 0.565% (curve A). Curve B is that for the fractional velocity change during recovery at constant strain (with load). Curves C and D are those for attenuation change and fractional velocity change, respectively, under no load.

The general form of the attenuation recovery, with or without load, is similar to that of the aluminum single crystals. On the other hand there are marked differences between the two types of velocity behavior for aluminum and sodium chloride. As seen in Figure (17) (curve D) the velocity initially does not change whereas in curve B there is a sharp drop followed by an increase approximately back to the starting point. Neither of these two types of recovery behavior has been found in aluminum. The recovery behavior in sodium chloride appears at present to be very different from that observed in aluminum.

Following recovery, that is seventy two hours later, the sodium chloride sample, for which the recovery has been shown, was reloaded until it broke at 1.39% strain. The stress-strain curve and the attenuation-strain curve are shown in Figure (18). The attenuation continued to increase with strain and without sign of a maximum until fracture occurred.

This work on sodium chloride has been started recently and relatively little data is available thus far. It is intended that measurements of conductivity and surface charge will be made as well as attenuation-strain and velocity strain measurements.

10

III.   Discussion of Preparations For Stress Cycling Single Crystals

Preparations for cyclic fatigue tests of single crystals of aluminum have progressed. This work has involved necessary changes in the cycling mechanism which consists of a servomechanism controlled universal testing machine and a programming device. A new load cell of the necessary low capacity for these tests has been installed and the required changes in circuitry made. A suitable amplifier and extensometers have also been provided to permit stress-strain recording. Three different avenues of approach have been under exploration for providing the desired triangular shaped cyclic load pattern in order to produce a more accurate loading cycle than previously achieved. There are problems of linearity and response rate, especially at the abrupt reversal in loading rate, with each of the three methods. None of these has been found to be entirely satisfactory.
The three methods are:
1.   A mechanically cycled elastic member containing resistance gages to provide the required modulated cycle for programming the machine.

2.   A clock motor-driven, continuously-rotating potentiometer with associated electronics.

3.   A commercially available electronic function generator.

Provision of suitable grips to hold the single crystal specimen in the testing machine without introducing undesired bending or clamping stresses is a different problem. The first design of these grips has proven to be unsatisfactory, and a second design incorporating features which will permit better adjustment of alignment has been prepared.

As this report is written the equipment in question is very nearly ready to try out on cycling a single crystal of aluminum.

11

IV.   Description of Automatic Recording Velocity Measurement System

An automatic recording velocity measurement unit has been developed and while a working model of the full unit is not yet in operation, various component sections of the unit have been tested. This unit will make it possible to record changes in round trip time of ultrasonic echoes. The unit has been planned to be practically insensitive to changes in repetition rate, pulsed oscillator jitter, pulse amplitude and rise time, and to changes in sample attenuation. One nanosecond (10^{-9}) changes in round trip time may be observed with a probable accuracy of $\pm$ 5%. It is expected that changes in time of 0.1 nanosecond (10^{-10}) will be observable. Expected accuracy for the measurement of 10 nanoseconds or greater is $\pm$ 1%. It is planned to make patent application for this device.

REFERENCES

1. "Fatigue and Ultrasonic Attenuation," by Rohn Truell and Akira Hikata
   Special Technical Publication #215, American Society for Testing Materials (1957)

2. "Fatigue Phenomenon in High Strength Aluminum Alloys," R. F. Hanstock
   Journal Institute of Metals 83, 11 (1954)

3. The Use of Ultrasonic Methods to Determine Fatigue Effects in Metals,"
   Rohn Truell, Bruce Chick, Amos Picker and George Anderson
   WADC Technical Report 59-389 (1959)

4. "The Use of Ultrasonic Methods for the Examination of Fatigue Effects in Metals
   During the Early Stages of Stress Cycling," Rohn Truell et al
   WADD Technical Report 60-920 (1960)

5. "Internal Friction Phenomena Due to Dislocations",
   Dislocations and Mechanical Properties of Crystals, Andrew Granato and Kurt Lucke
   425 John Wiley and Sons, Inc. (1957)

6. "Sensitivity of Ultrasonic Attenuation and Velocity Changes Due to Plastic
   Deformation",Akira Hikata, Rohn Truell, Bruce Chick and Kurt Lucke
   Journal of Applied Physics 27, 396 (1956)
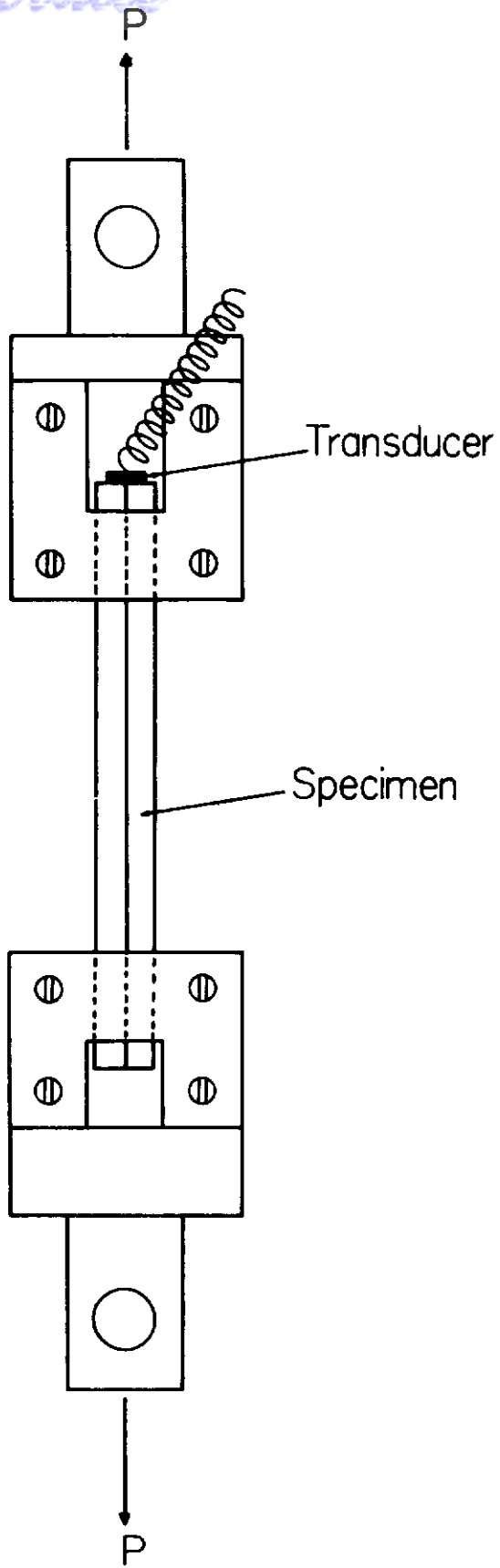
Figure 1
Specimen Holder (Schematic)

14

to load cell

Dial Indicator

Specimen

Crosshead
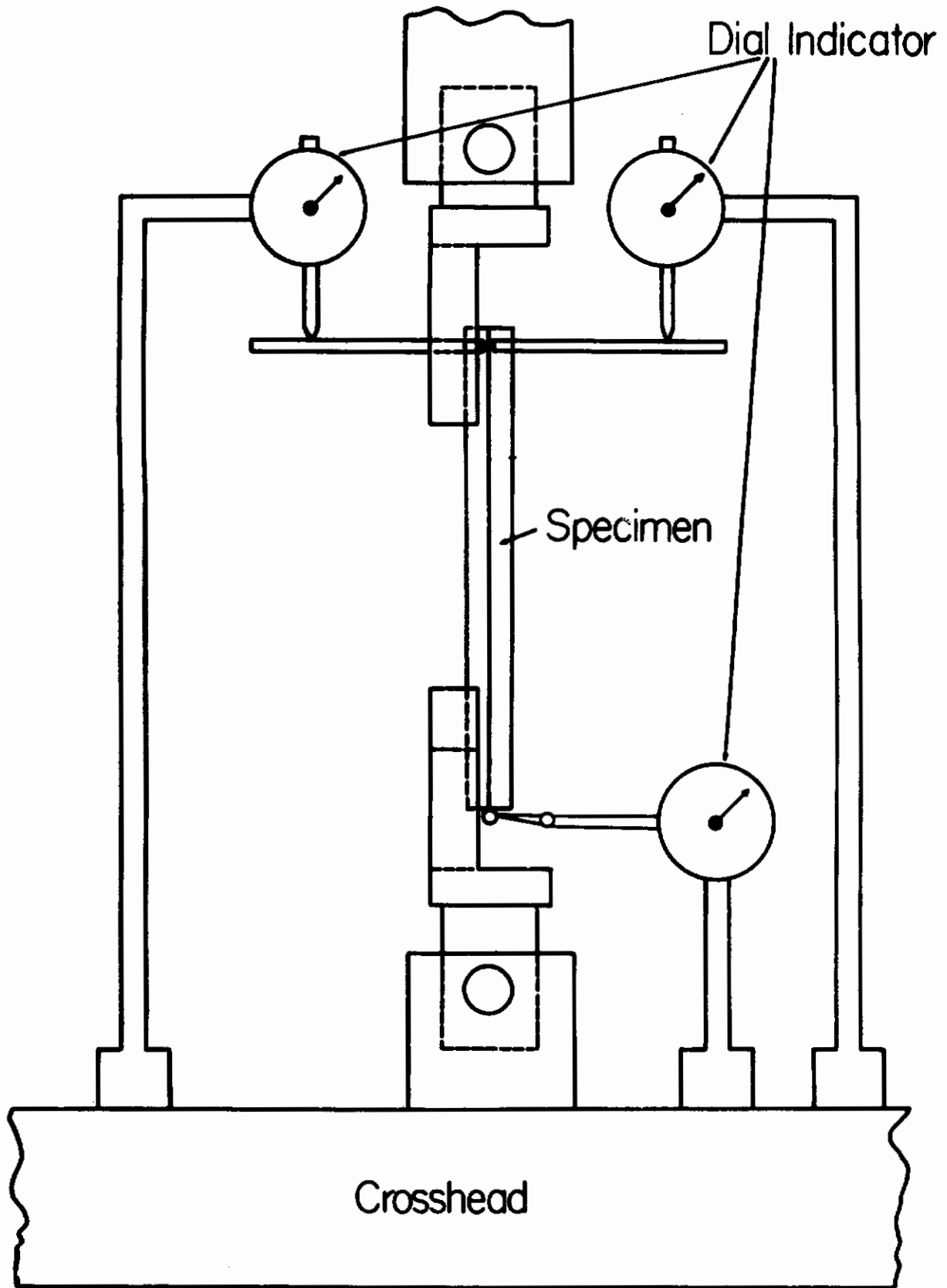
Figure 2.
Elongation Measurement Equipment

15
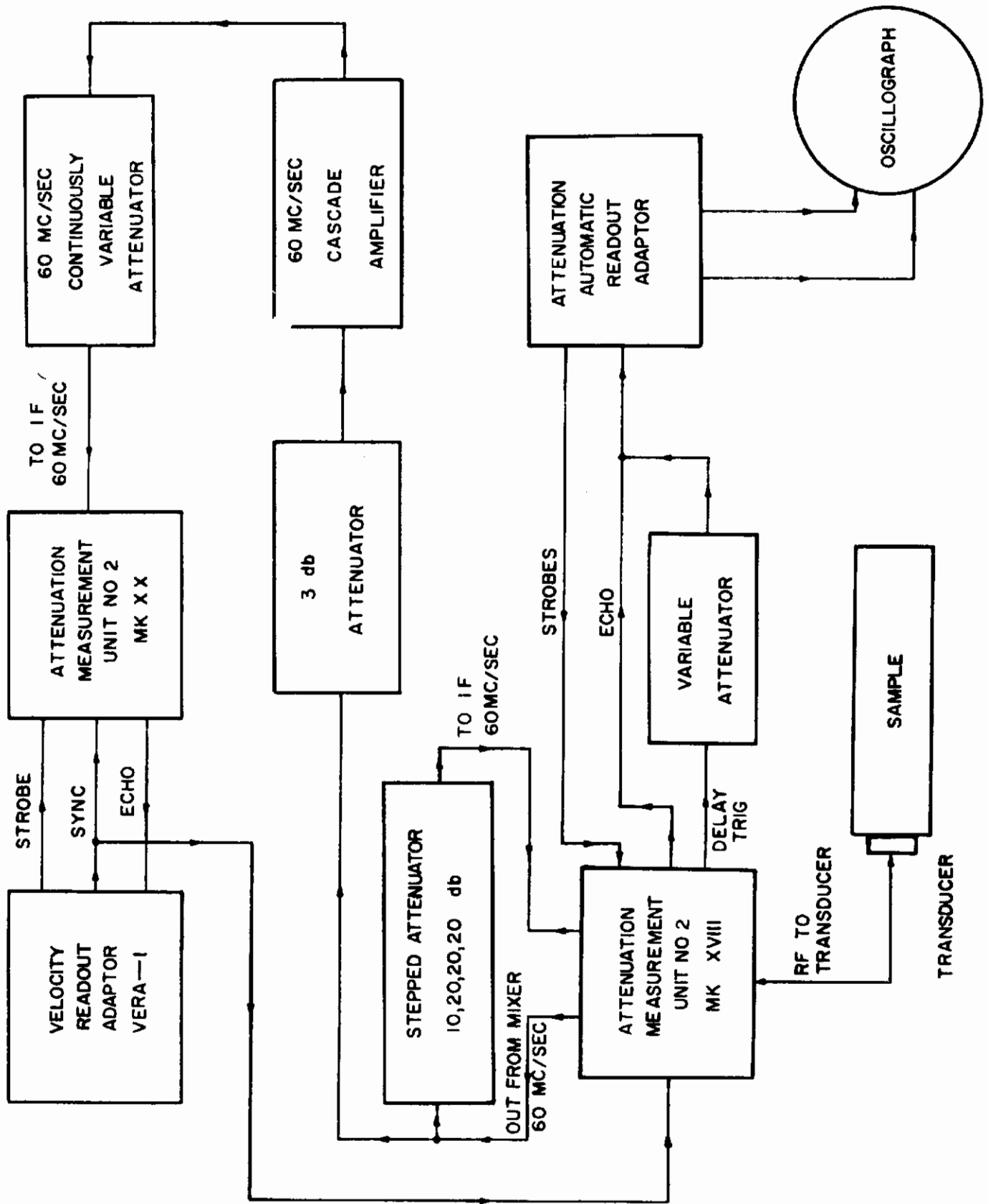
Figure 3.
Automatic Recording Attenuation Equipment

Aluminum Single Crystal
Initial Attenuation 0.0214 db/μsec
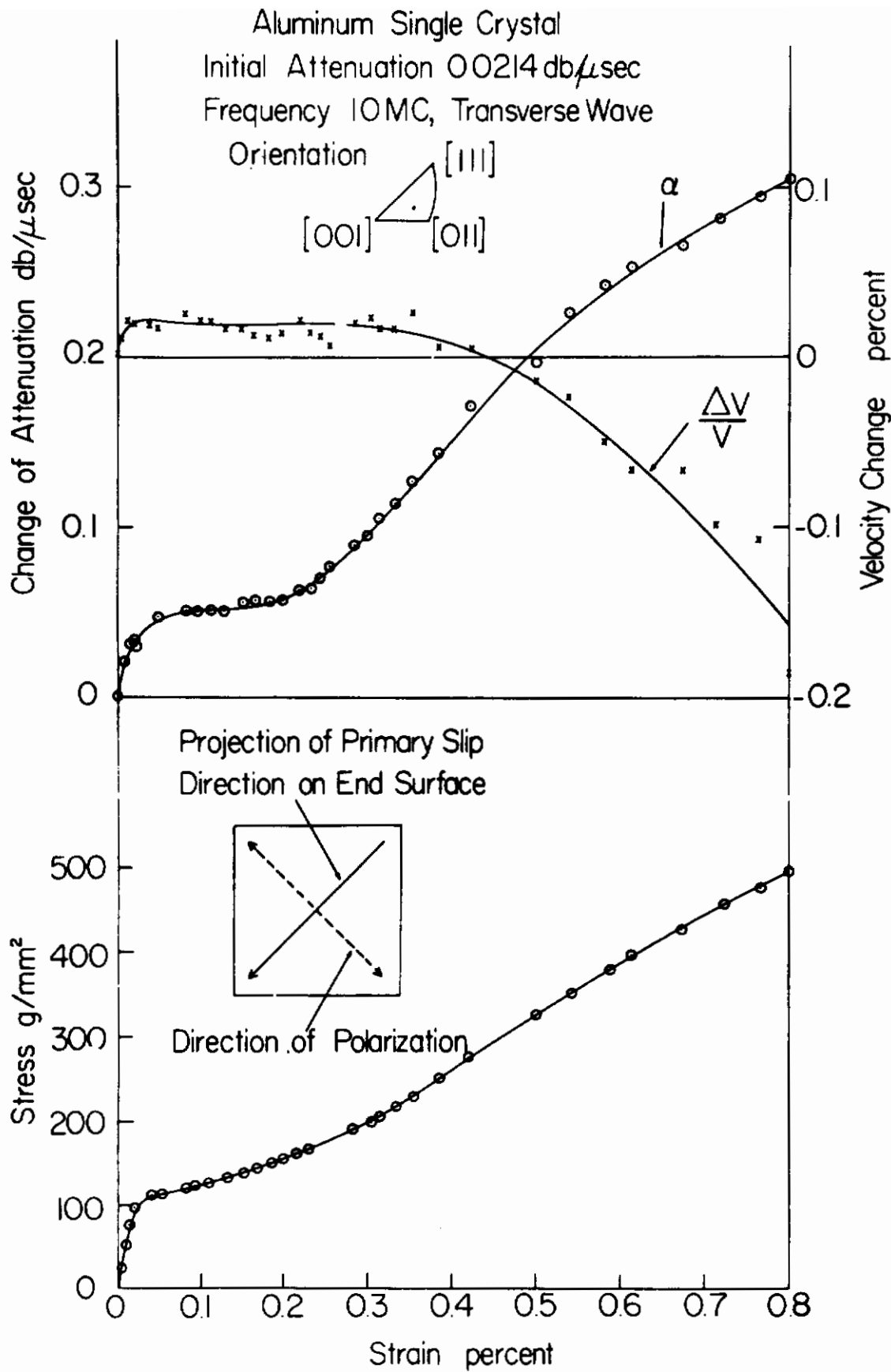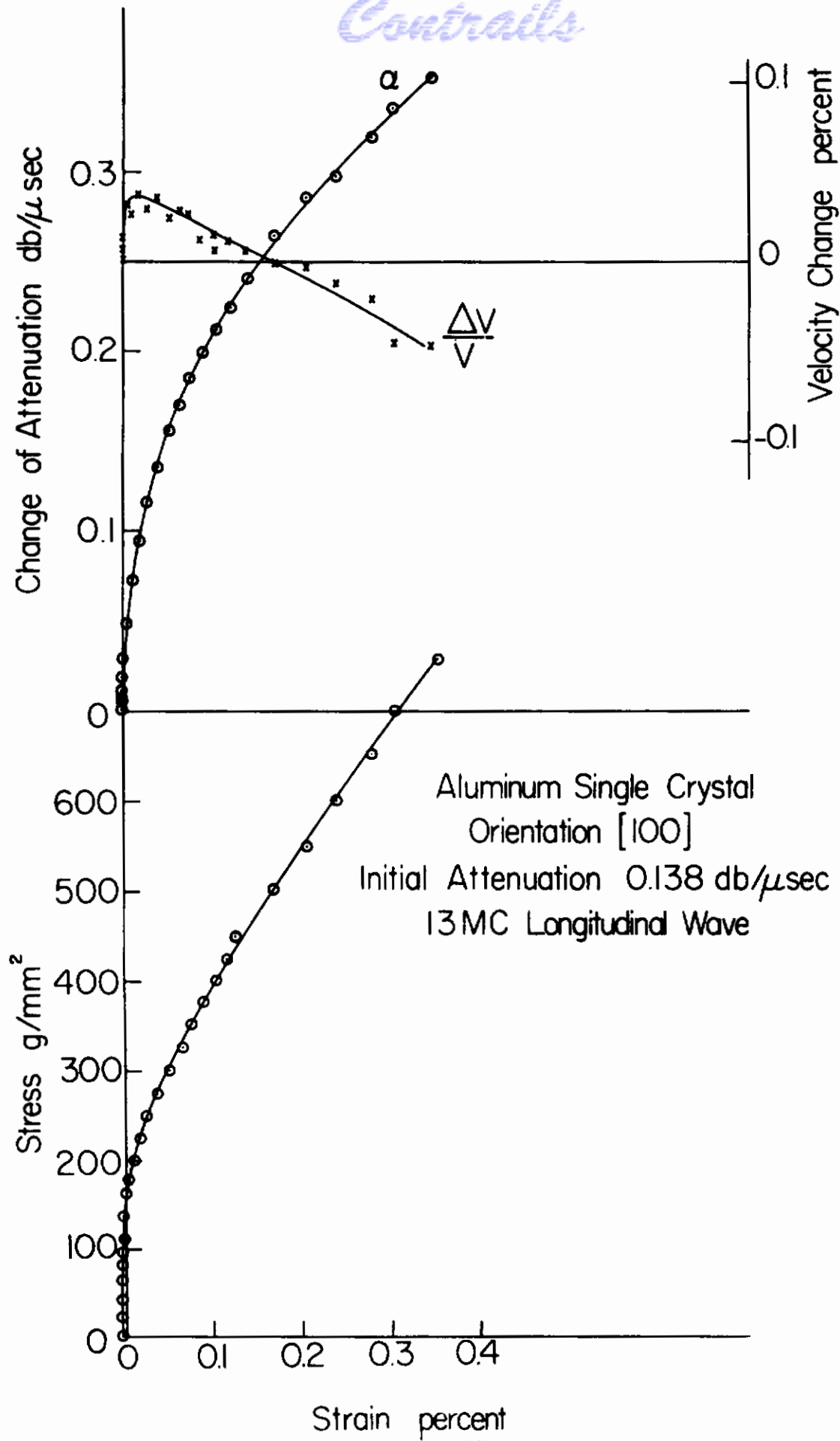Frequency 10 MC, Transverse Wave
Orientation

Figure 4.
Stress, Shear Wave Attenuation And Velocity Change As a Function Of Total Strain
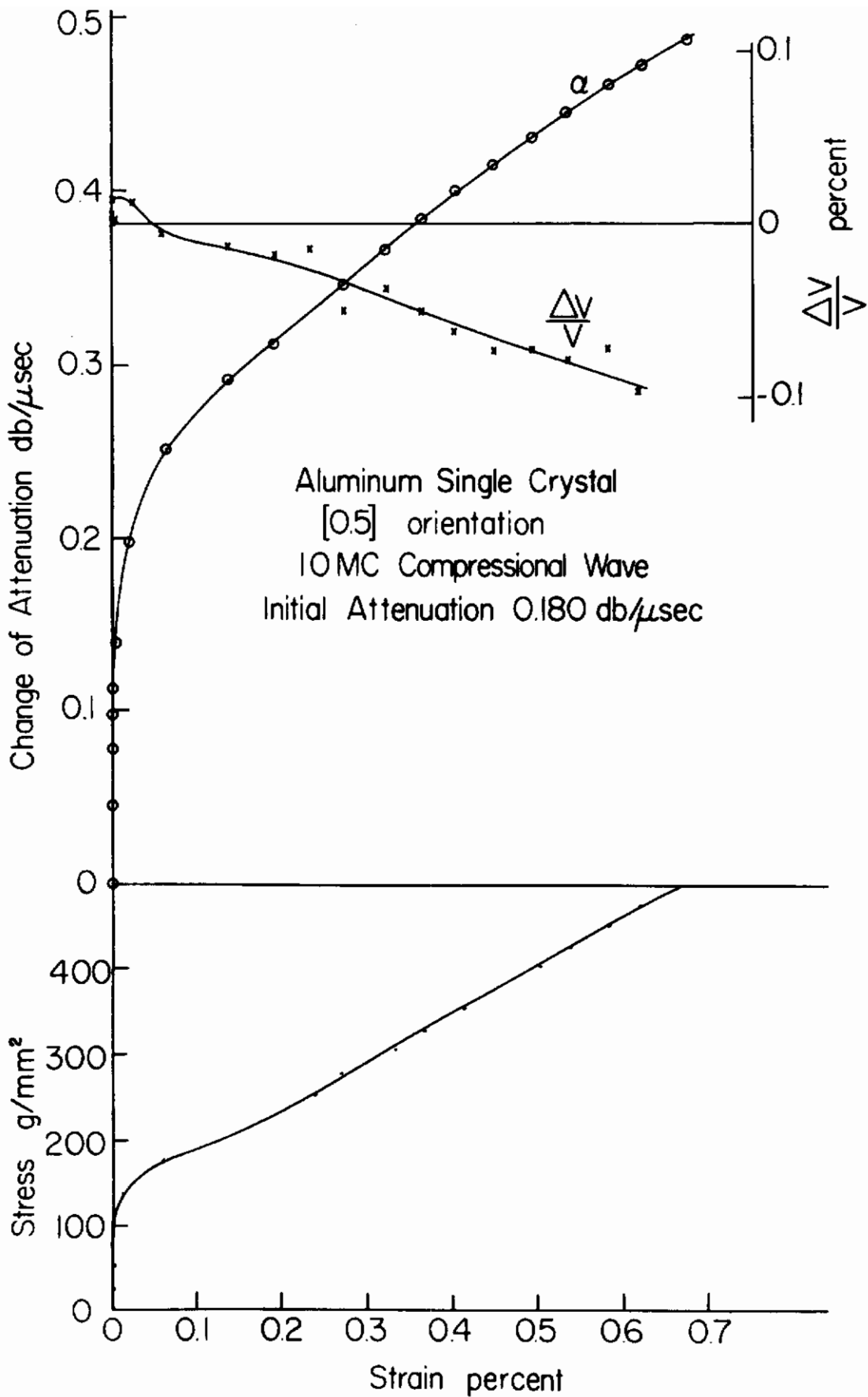
Figure 5.
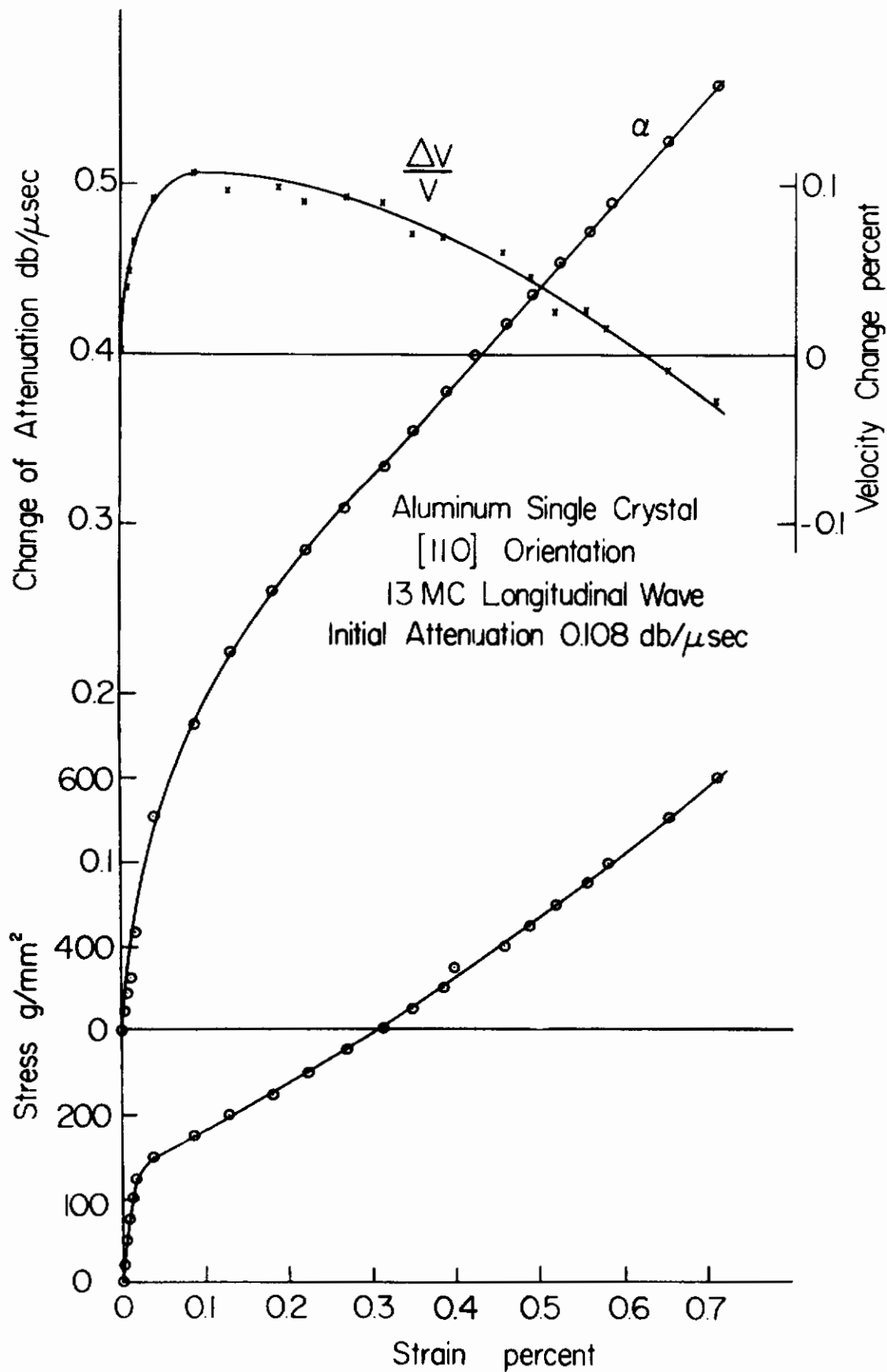Stress, Compressional Wave Attenuation and Velocity Change As A Function Of Total Strain

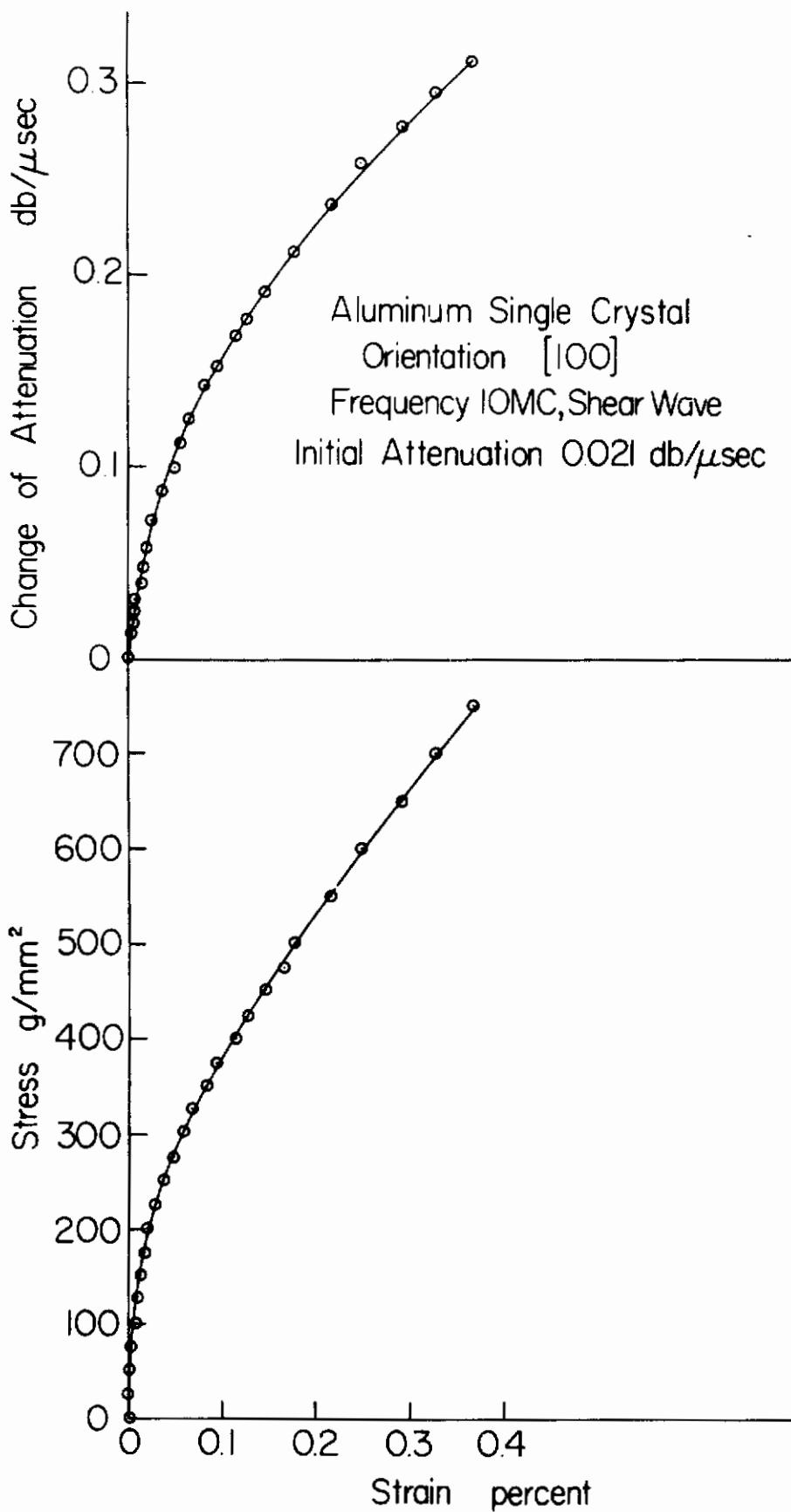Aluminum Single Crystal
[0.5] orientation
10 MC Compressional Wave
Initial Attenuation 0.180 db/μsec

18

Figure 6.
Stress, Longitudinal Wave Attenuation And Velocity Change As A Function Of Total Strain

Aluminum Single Crystal
Orientation [100]
Initial Attenuation 0.138 db/μsec
13 MC Longitudinal Wave

19

Aluminum Single Crystal
Orientation [111]
13 MC Compressional Wave
Initial Attenuation 0073 db/μsec
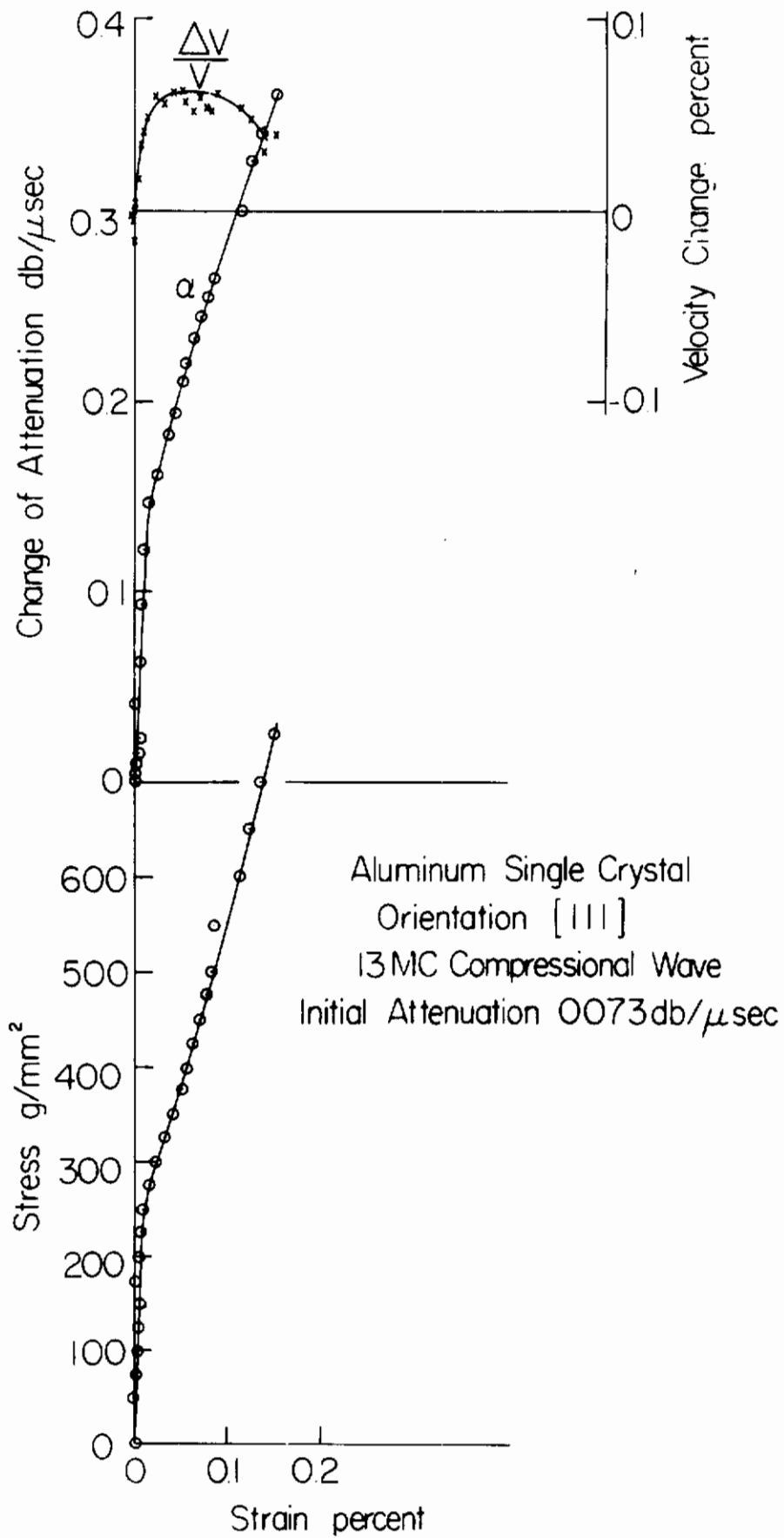
Figure 7.
Stress, Compressional Wave Attenuation And Velocity Change As A Function Of Total Strain

Figure 8.
Stress, Longitudinal Wave Attenuation And Velocity Change As A Function Of Total Strain

Aluminum Single Crystal
[110] Orientation
13 MC Longitudinal Wave
Initial Attenuation 0.108 db/μsec

Aluminum Single Crystal
Orientation [100]
Frequency IOMC, Shear Wave
Initial Attenuation 0.021 db/μsec

Figure 9.
Stress And Shear Wave Attenuation As A Function Of Total Strain

Aluminum Single Crystal
[110] Orientation
Initial Attenuation 0.0247 db/μsec
Polarization [1̄10]
10 MC Shear Wave
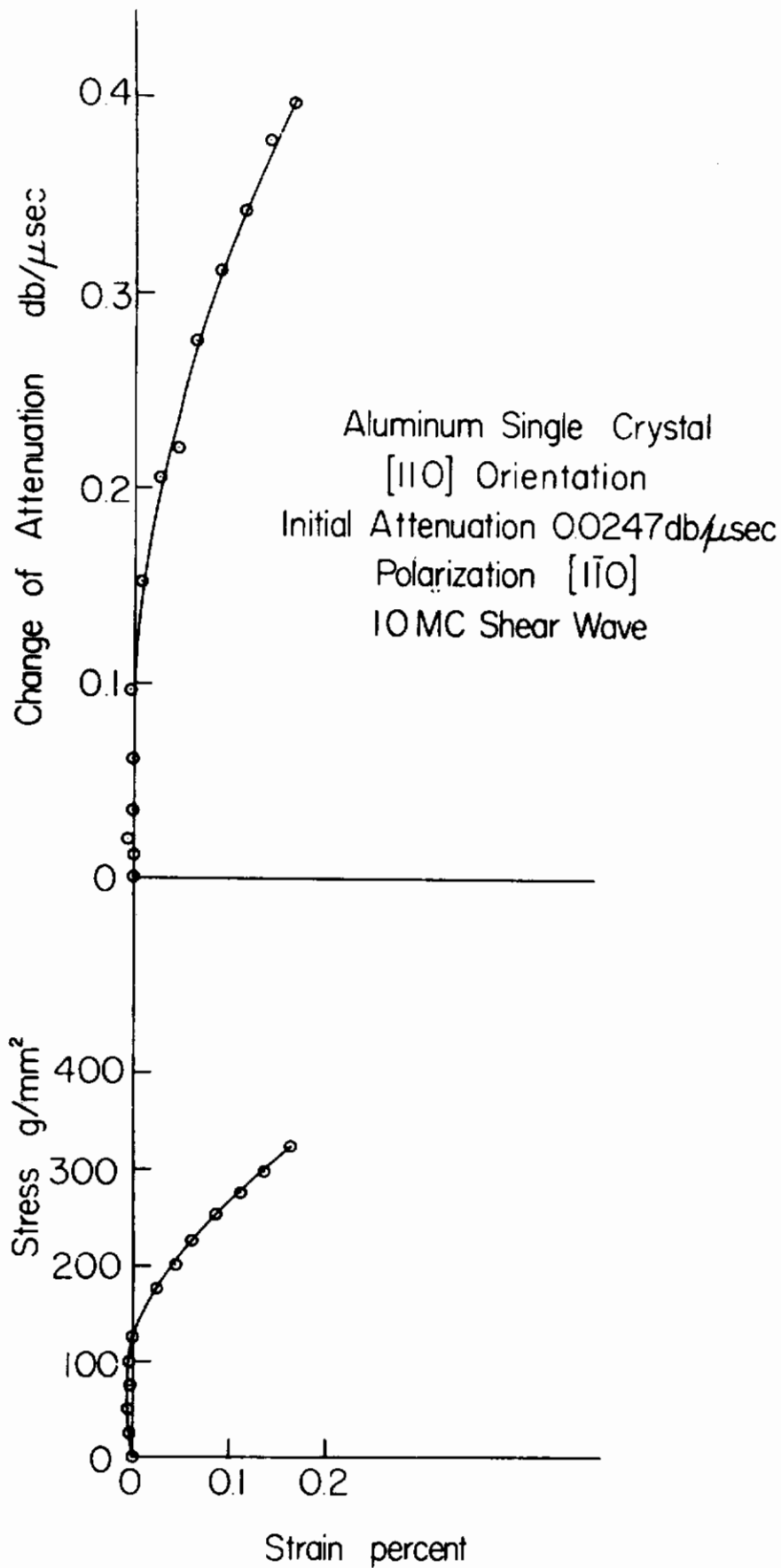
Figure 10.
Stress And Shear Wave Attenuation As A Function Of Total Strain

23

$$\alpha = K_1 \frac{1}{[(\Omega^2 - 1)^2 + (\frac{d}{\omega})^2]}$$

$$\frac{\Delta G}{G} = \frac{G(\omega) - G}{G} = K_2 \frac{(1 - \Omega^2)}{[(\Omega^2 - 1)^2 + (\frac{d}{\omega})^2]}$$

$$\Omega = \frac{\omega_0}{\omega} \qquad \omega_o = \frac{\pi}{L}(\frac{C}{A})^{\frac{1}{2}}$$

$$d = \frac{B}{A} \qquad C = \frac{2Ga^2}{\pi(1-\nu)}$$

$$A = \pi \rho a^2$$
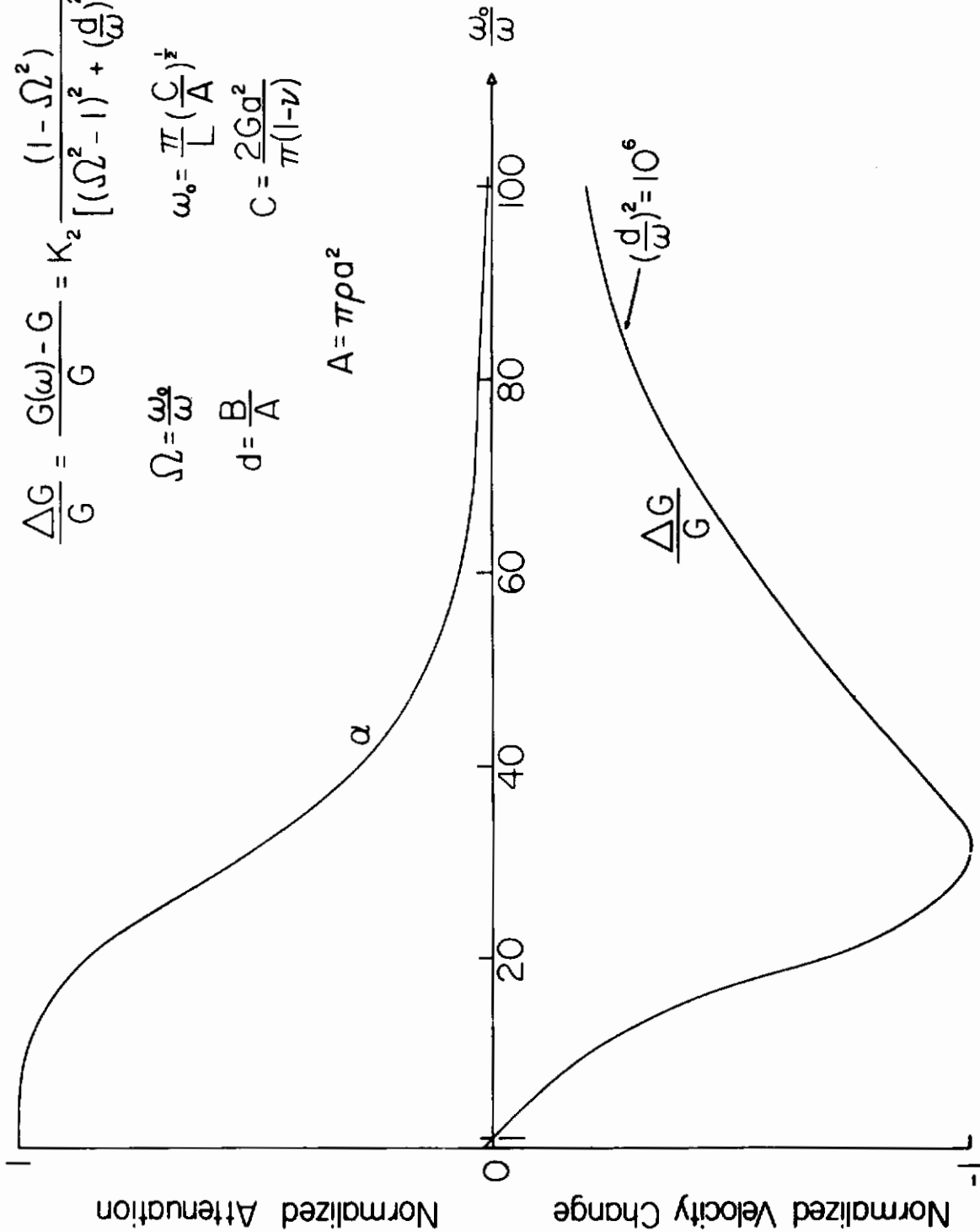
Figure 11.
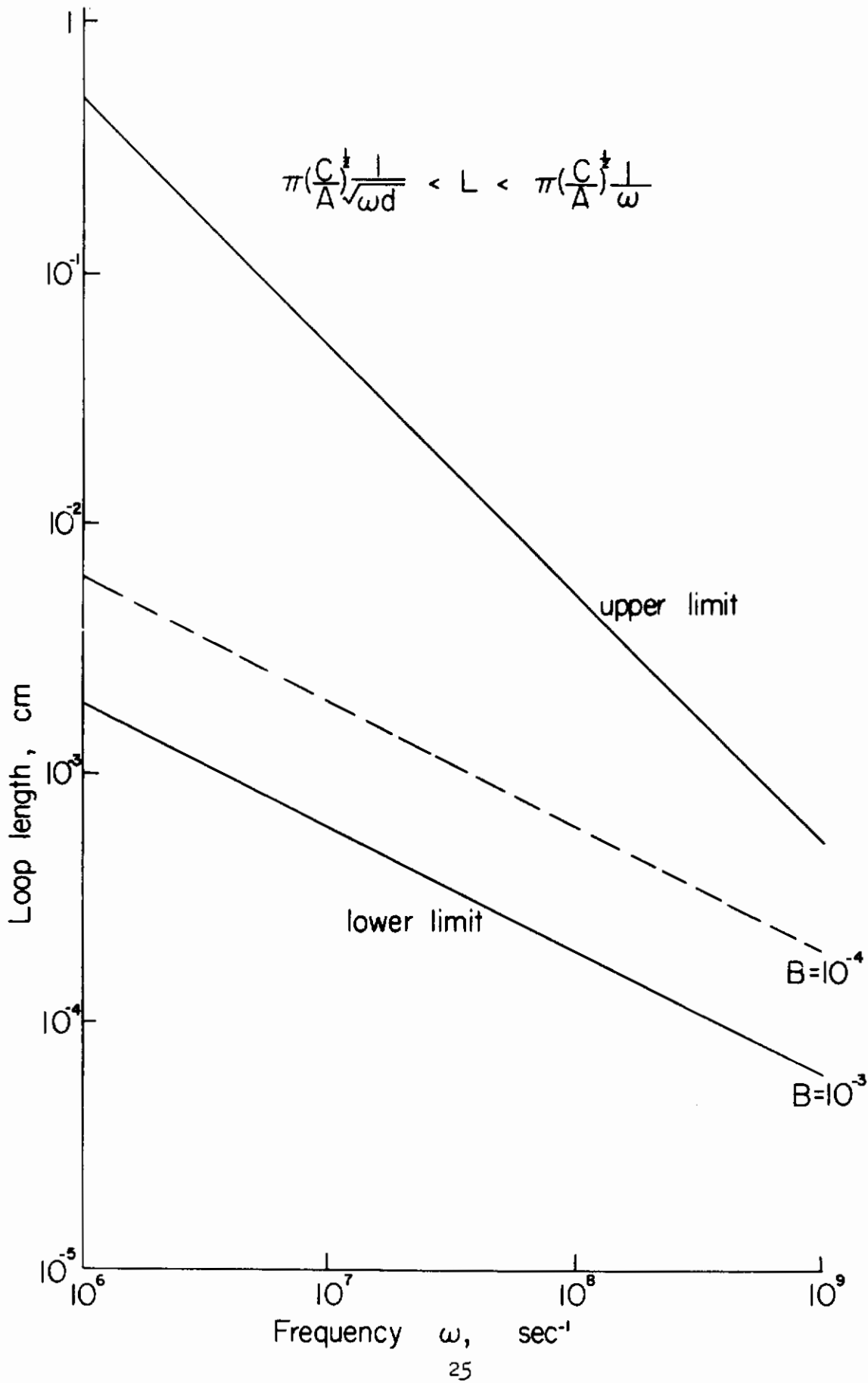Normalized Attenuation And Velocity Change As A Function Of Resonant Frequency

24

$$\pi\left(\frac{C}{A}\right)^{\frac{1}{2}}\frac{1}{\sqrt{\omega d}} \; < \; L \; < \; \pi\left(\frac{C}{A}\right)^{\frac{1}{2}}\frac{1}{\omega}$$

upper limit

lower limit

$B=10^{-4}$

$B=10^{-3}$

Loop length, cm

Frequency ω, sec^{-1}

Figure 12.
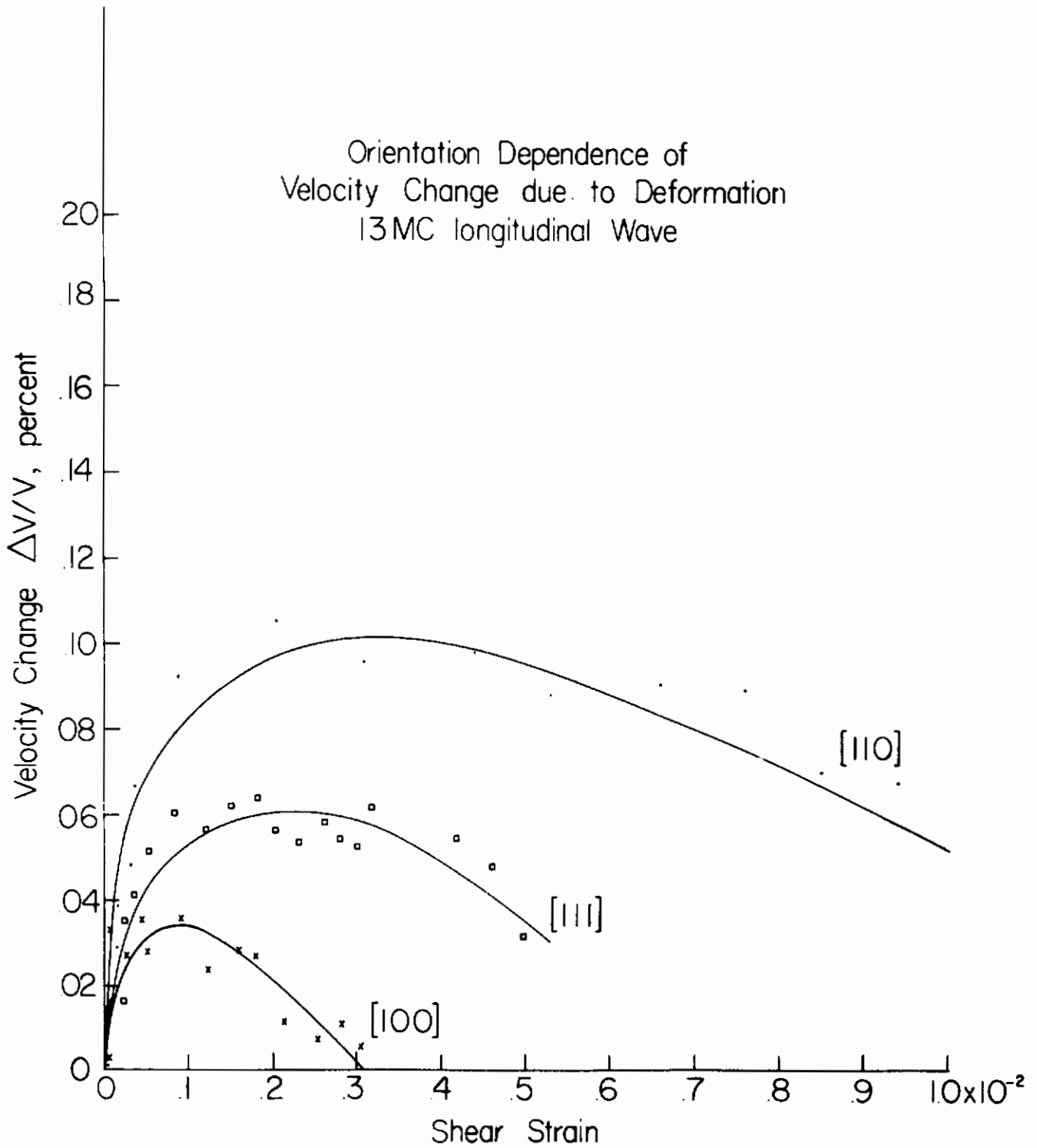Upper And Lower Limits On Loop Lengths As A Function Of Frequency

25

Figure 13.
Longitudinal Wave Velocity Change As A Function Of Shear Strain For The Orientations Indicated

26

Orientation Dependence of
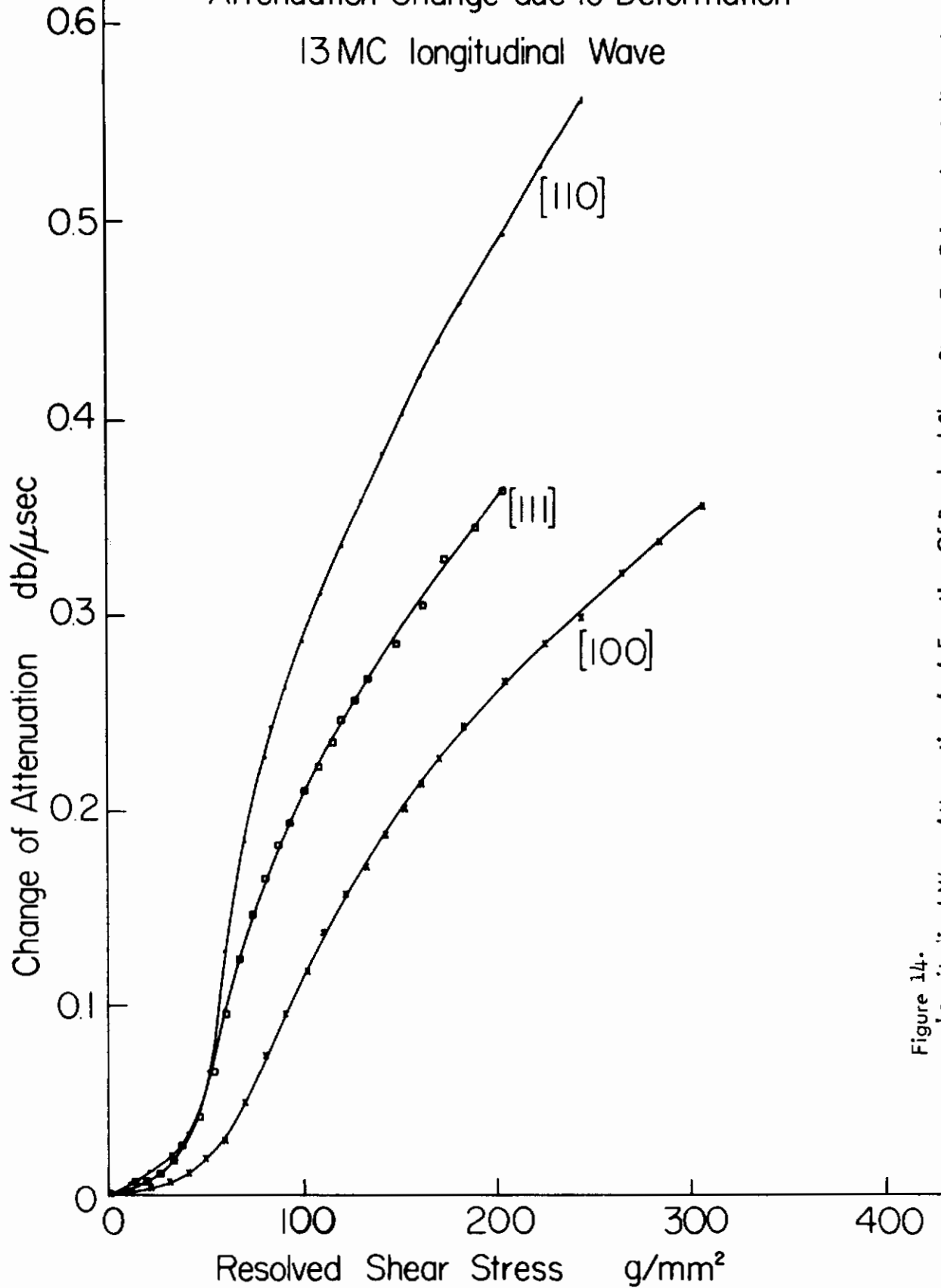Attenuation Change due to Deformation

13 MC longitudinal Wave

Figure 14.
Longitudinal Wave Attenuation As A Function Of Resolved Shear Stress For Orientations Indicated
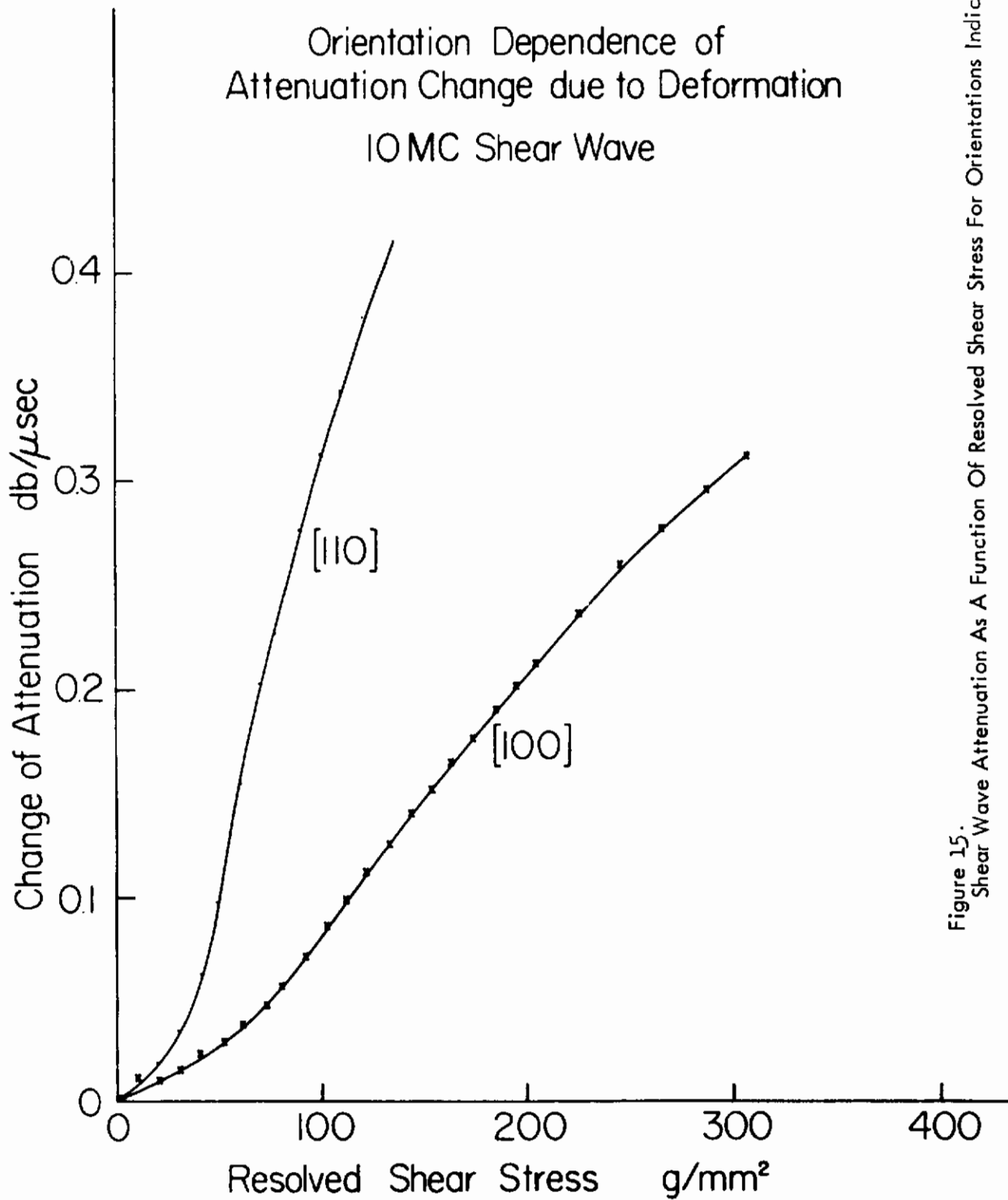
Orientation Dependence of
Attenuation Change due to Deformation

10 MC Shear Wave

Figure 15.
Shear Wave Attenuation As A Function Of Resolved Shear Stress For Orientations Indicated
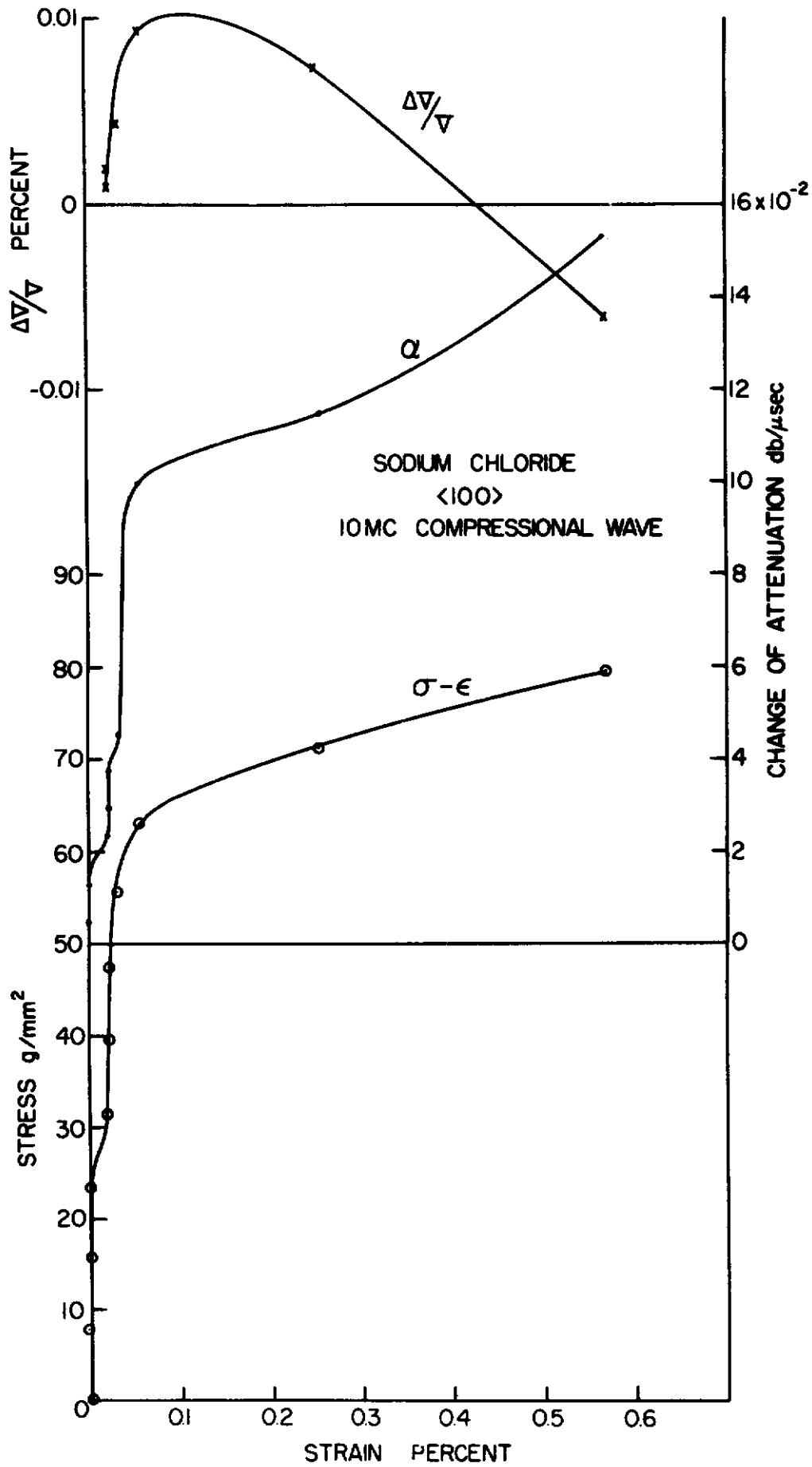
Figure 16.
Stress, Attenuation, And Velocity Change As A Function Of Total Strain
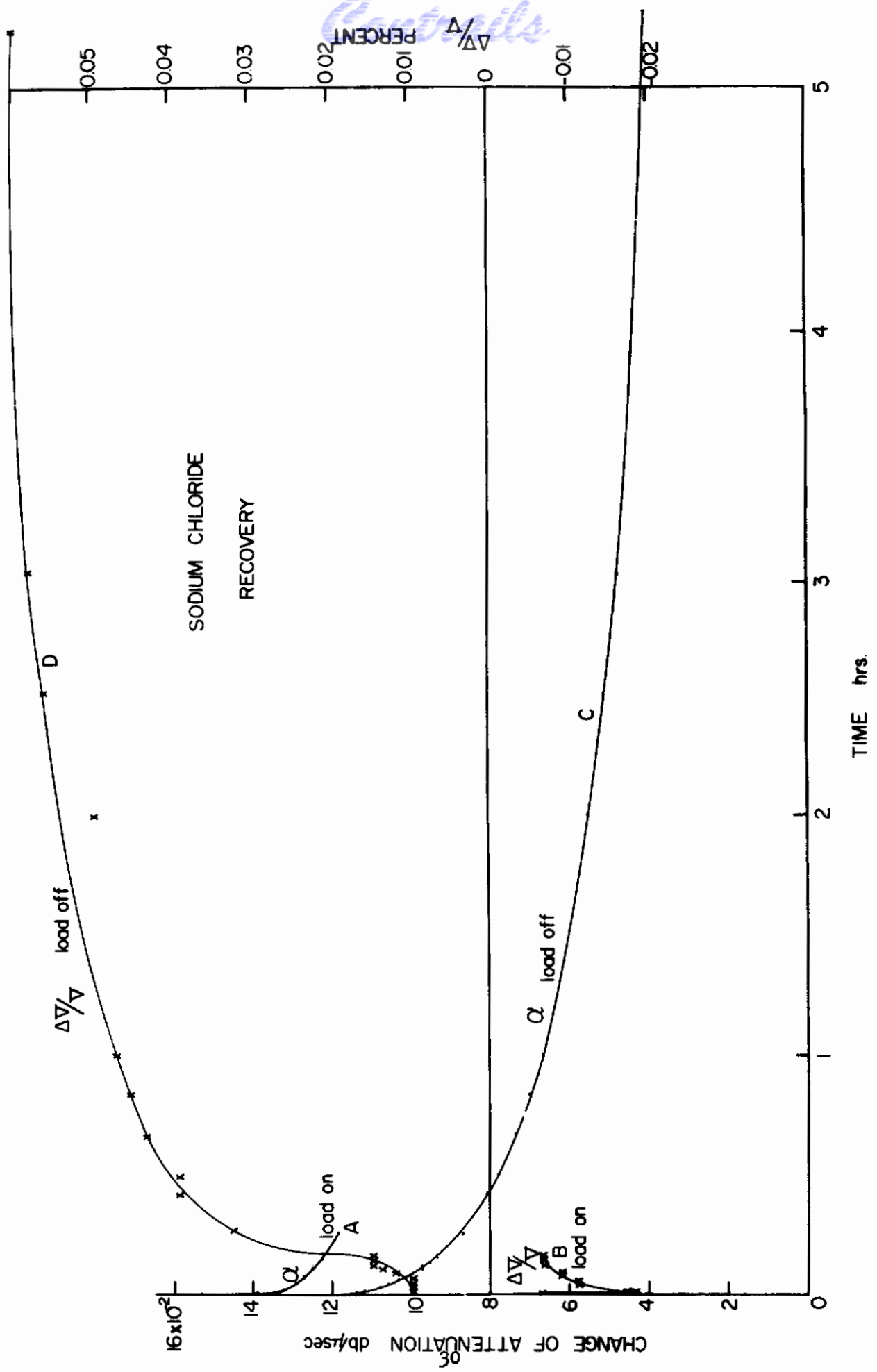
SODIUM CHLORIDE
<100>
10 MC COMPRESSIONAL WAVE

$\Delta V/V$

α

$\sigma - \epsilon$

29

Figure 17.
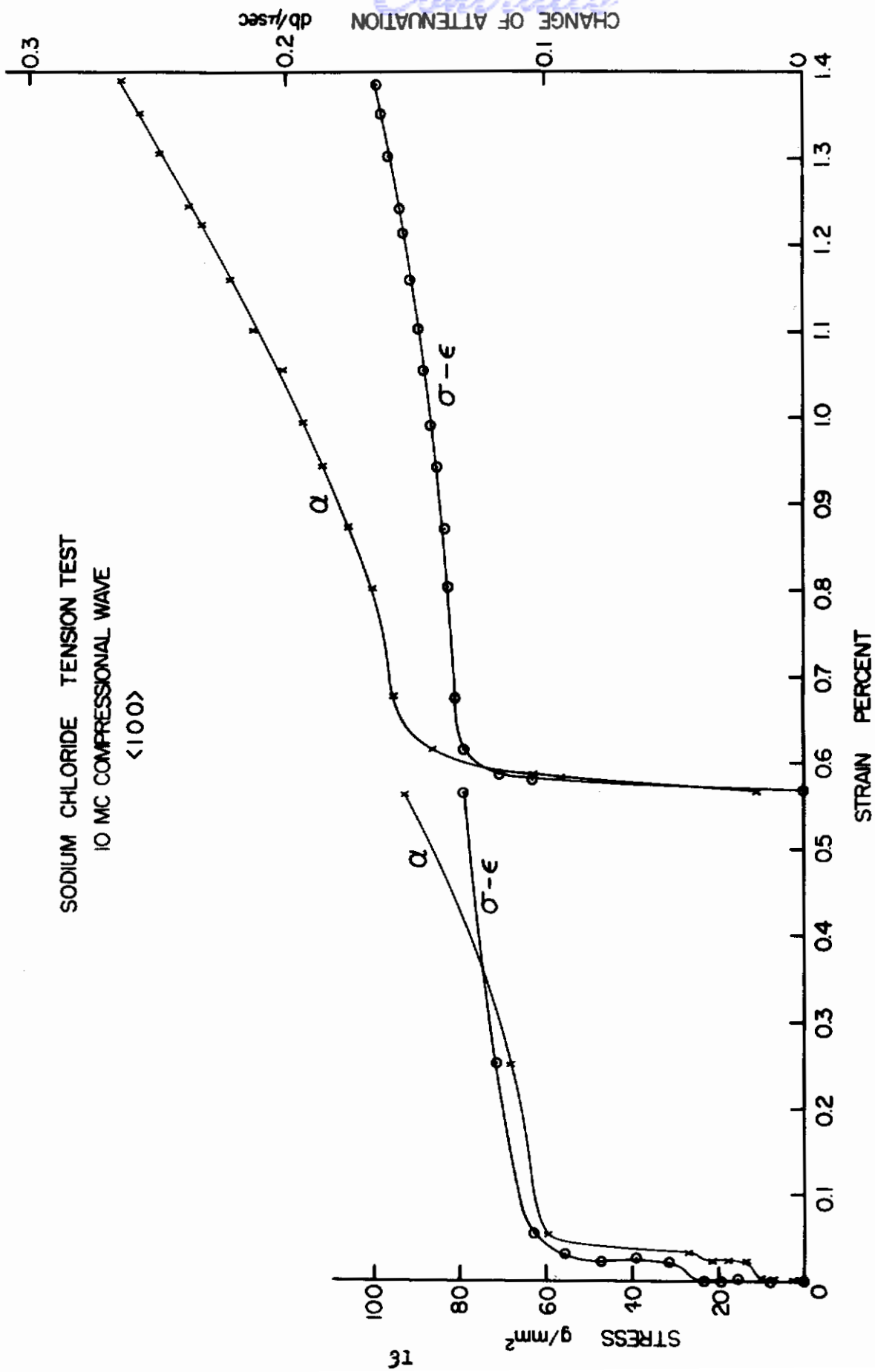Recovery Of Attenuation And Velocity With And Without Load

Figure 18.
Stress And Attenuation As A Function Of Strain For Two Successive Cycles Of Deformation

SODIUM CHLORIDE TENSION TEST
10 MC COMPRESSIONAL WAVE
<100>